ELSEVIER

Journal of Nuclear Materials 290–293 (2001) 825–828

journal of nuclear materials

www.elsevier.nl/locate/jnucmat

Pumping effect on the divertor plasma and detachment in the JT-60U W-shaped divertor

N. Asakura *, S. Sakurai, H. Tamai, Y. Koide, Y. Sakamoto, O. Naito, H. Kubo, K. Itami, K. Masaki

Naka Fusion Research Establishment, Japan Atomic Energy Research Institute Naka-machi, Naka-gun, Ibaraki-ken 311-01, Japan

Abstract

Effects of the divertor pumping on the SOL plasma flow and neutral recycling were investigated under high density and detached divertor conditions, using reciprocating Mach probes at the outer midplane and just below the divertor x-point. For the divertor pumping from inner and outer sides of the private dome (both-sides pumping), plasma flow in the outer divertor was increased compared to that for the inner-side pumping case (i.e., closing the outer pumping slot) when the plasma detachment appeared on the divertor target. Partially detached plasma was maintained at the inner and outer divertor without causing x-point MARFE, and in–out symmetrical profiles of D_α brightness and ion flux were observed. © 2001 Elsevier Science B.V. All rights reserved.

Keywords: JT-60U; Plasma flow; Divertor pumping

1. Introduction

Control of the plasma flow in the scrape-off layer (SOL) and divertor, using a divertor pumping system, is considered important because of its implications for the helium exhaust and impurity retention in the divertor [1]. Understanding effects of the divertor pumping on the SOL plasma and neutral recycling is a critical issue to design the divertor geometry and pumping system efficient for a tokamak reactor. Experimental results have been obtained in various divertor geometries and pumping slot locations [2–5]. However, there were few measurements of the SOL plasma flow with changing divertor pumping rate, and the effect on the plasma flow pattern is not understood.

In JT-60U, a pumping slot in the outer side of the W-shaped divertor was opened since 1999, and pumping from the private flux region in the inner and outer divertors (both-sides pumping) has been used to increase effective pumping rate for high density and detached divertor operations. In this paper, the SOL plasma flow for the cases of gas puff at plasma top and pumping at the down-stream side (divertor private flux region) is investigated using the reciprocating Mach probes installed at two important locations (i.e., the outer midplane and the x-point) [6]. Effect of bypath between the inner and outer divertors under a dome on the particle recycling is also studied.

2. Plasma flow in SOL and divertor

Profiles of electron temperature (T_e) and ion saturation current (j_s) in the SOL were measured in the L-mode plasmas, where $I_p = 1.6$ to 1.7 MA, $B_t = 3.5$ T, $q_{95} = 3.5$ and the ion ∇B drift direction towards the divertor. The direction of the plasma flow along the field lines is deduced from the ratio of j_s at the down-stream side (divertor side) of the Mach probe to j_s at the up-stream side (midplane side), i.e., $j_{s,down}/j_{s,up}$. A value lower than unity indicates a normally directed flow from the up-stream to the down-stream location along the field lines. A value larger than unity corresponds to a flow directed away from the divertor (i.e., 'flow reversal').

* Corresponding author. Tel.: +81-29 270 7613; fax: +81-29 270 7339.

E-mail address: asakuran@fusion.naka.jaeri.go.jp (N. Asakura).

PII: S 0 0 2 2 - 3 1 1 5 (0 0) 0 0 5 3 8 - 9

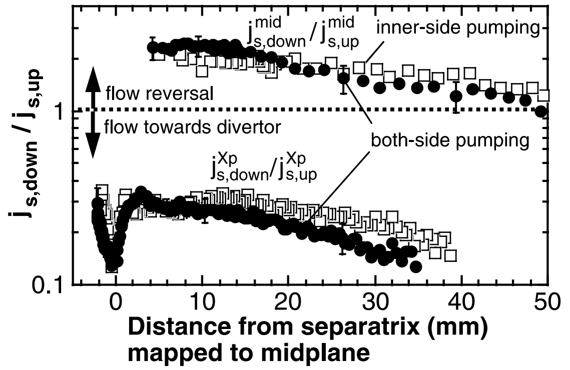

Fig. 1. Ratios of ion saturation current at midplane, and near the x-point, for the inner-side pumping (squares) and the both-side pumping (circles). For this experiment, $\bar{n}_e = 1.8 \times 10^{19}\ \mathrm{m}^{-3}$. Profiles for the x-point Mach probe are mapped to the same field lines at the midplane radius.

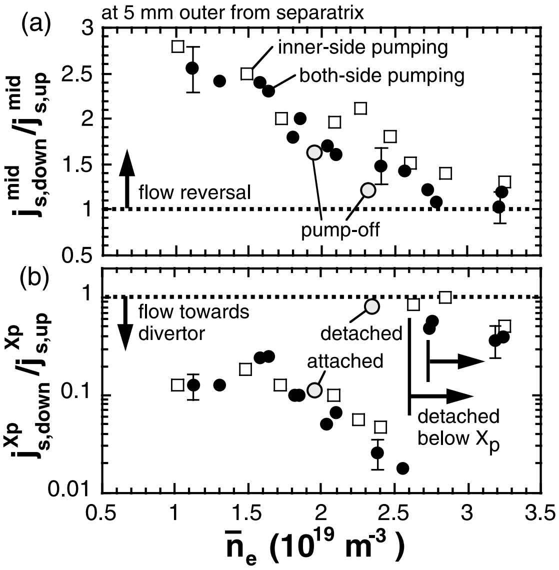

Fig. 2. Ratios of $j^{mid}_{s,down}/j^{mid}_{s,up}$ and $j^{Xp}_{s,down}/j^{Xp}_{s,up}$ near the separatrix as a function of $\bar{n}_e$ for the inner-side pumping (squares) and the both-sides pumping (circles). These for both-sides pumping slots but without divertor pumping (pump-off) is shown by gray circles.

Profiles of j_s ratios at the midplane and just below the x-point, $j^{mid}_{s,down}/j^{mid}_{s,up}$ and $j^{Xp}_{s,down}/j^{Xp}_{s,up}$, are shown in Fig. 1. The profiles for the both-sides pumping are compared with those for the inner-side pumping alone, where the pumping slot in the outer divertor (at the down-stream of the probe) is closed. The profiles of j_s ratio are comparable both at the midplane and near x-point for the relatively low main plasma density, $\bar{n}_e$: flow reversal occurs at the midplane, while the plasma flows from the x-point to the divertor plate. A mechanism to produce the flow reversal at the midplane has been proposed based on the in–out asymmetry in the ion poloidal drift velocity in a torus [7], and the model is consistent with the experimental results, i.e., the flow reversal is decreased at high density. Plasma flow near the x-point is driven towards the divertor target, which is a plasma sink under attached divertor conditions.

The j_s ratios at 5 mm outer from separatrix are shown versus increasing $\bar{n}_e$ in Fig. 2. With increasing $\bar{n}_e$, the flow reversal at the midplane decreases and the plasma flow just below the x-point increases (i.e., $j^{Xp}_{s,down}/j^{Xp}_{s,up}$ decreased) under conditions in which the attached plasma is maintained at the x-point ($\bar{n}_e \leqslant 2.55 \times 10^{19}\ \mathrm{m}^{-3}$). For the both-sides pumping, the divertor plasma flow tends to increase at high density of $\bar{n}_e = (2.0–2.55) \times 10^{19}\ \mathrm{m}^{-3}$, i.e., $j^{Xp}_{s,down}/j^{Xp}_{s,up}$ of 0.02–0.03 is smaller than $j^{Xp}_{s,down}/j^{Xp}_{s,up}$ of 0.05–0.06 for the inner-side pumping alone. At the same time, small reduction of the reversal flow is observed at midplane. In these experiments, the gas puff rate is determined by feed-back control to maintain the pre-programmed density. The rate is increased up to 22–25 Pa $\mathrm{m}^3\ \mathrm{s}^{-1}$, which is comparable for the two cases. These facts suggest that the increase in the plasma flow at the divertor by the both-sides pumping is relatively small so that the plasma flow pattern in the main plasma edge does not change. The ion poloidal drift rather than the parallel flow may produce net plasma flow at the main plasma edge. Another candidate is that the increment of the plasma flow at the outer divertor is compensated by a reduction in that at the inner divertor.

3. Pumping effect on divertor detachment

Electron pressure profiles at the up-stream and down-stream of the outer divertor, p^{Xp}_e, $p^{div}_{e,out}$, and at the inner divertor, $p^{div}_{e,in}$, are shown in Fig. 3 with increasing $\bar{n}_e$ from 1.8×10^{19} to $2.8 \times 10^{19}\ \mathrm{m}^{-3}$ for the both-sides pumping. Improvement of the divertor operation is observed for the both-sides pumping case: partially detached plasma at both divertor targets without causing the x-point MARFE (and plasma detached below the x-point) is maintained as shown by closed circles, providing that $\bar{n}_e$ is kept in the adequate range of $(2.3–2.55) \times 10^{19}\ \mathrm{m}^{-3}$. Greenwald density fraction, $\bar{n}_e/n^{Gr}$, corresponds to 0.46–0.52, where $n^{Gr} \times 10^{20}\ \mathrm{m}^{-3} \equiv I_p/\pi a_p^2\ [\mathrm{MA\ m^{-2}}]$ and a_p is the minor radius at the midplane. For the inner divertor pumping, plasma detachment at both divertor sides is observed only at $\bar{n}_e \sim 2.45 \times 10^{19}\ \mathrm{m}^{-3}$, and the x-point MARFE appears at higher $\bar{n}_e$.

Values of p^{Xp}_e and $2p^{div}_{e,out}$ at the separatrix for the both-sides pumping case are compared to those for the inner-side pumping case in Fig. 4. With increasing $\bar{n}_e$

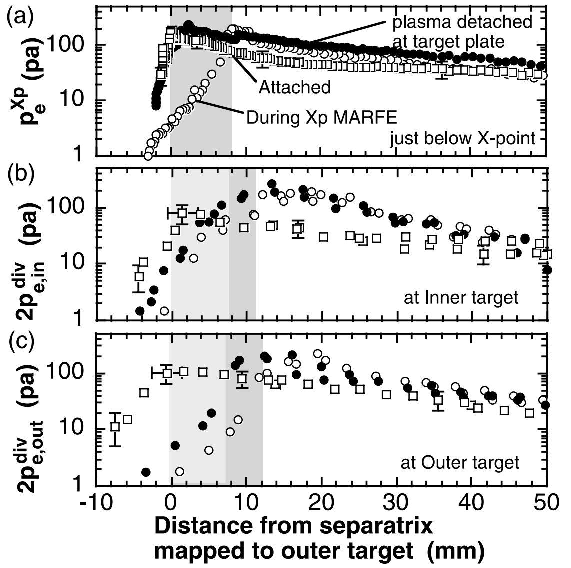

Fig. 3. Electron pressure profiles: (a) below the *x*-point; (b) at the inner divertor; and (c) at the outer divertor for the three cases: attached divertor, detached divertor on the inner and outer targets, and during *x*-point MARFE. For these experiments, $\bar{n}_e = 1.8$, 2.4 and 2.75×10^{19} m^{-3}, respectively. Profiles of (a) and (b) are mapped to the same field lines at the outer target.

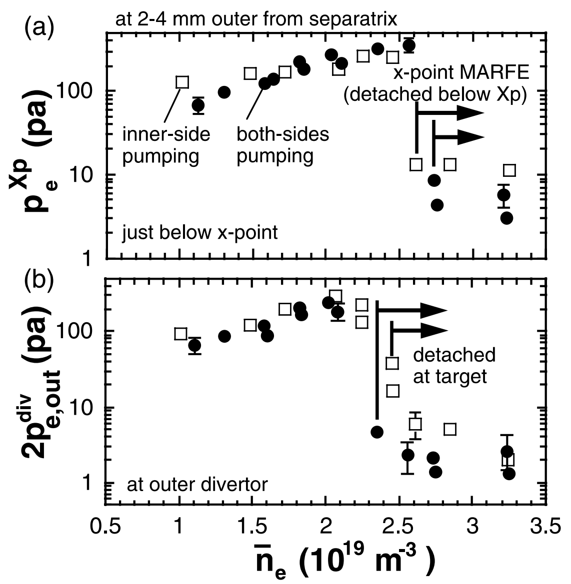

Fig. 4. Comparisons of: (a) p_e^{Xp}; (b) $2p_{e,out}^{div}$ at the outside separatrix as a function of $\bar{n}_e$ for both-sides pumping (circles) and inner-side pumping (squares).

from 2.38×10^{19} to 2.55×10^{19} m^{-3}, T_e^{Xp} decreases from ~60 to 10–30 eV, while p_e^{Xp} is maintained at 230–340 Pa. These values are comparable for the inner-side and both-sides pumping cases. In contrast, $2p_{e,out}^{div}$ for the both-sides pumping case decreases to $(0.01–0.02)p_e^{Xp}$, i.e., plasma detachment occurs at the target plate. The ratio is smaller than 0.05–0.1 for the inner-side pumping case. The difference of $2p_{e,out}^{div}/p_e^{Xp}$ is mostly due to a large reduction in the ion flux at the divertor, while T_e^{div} of ~5 eV is comparable.

The larger plasma flow below the *x*-point for the both-sides pumping, compared to that for the inner-side pumping at the same $\bar{n}_e$, is produced by larger reduction in $p_{e,out}^{div}$. Neutral source at the separatrix is presumably reduced by the divertor pumping from the private flux region. The larger reduction in $p_{e,out}^{div}$ is also observed during the *x*-point MARFE, where T_e^{Xp} decreases to 3–4 eV and the detachment region extends to the up-stream (*x*-point), and at the same time extends to the outer flux surfaces (width of ~1.5 cm at the target) as shown by open circles in Fig. 3.

The neutral density in the private flux region is increased by gas puff from the divertor (divertor-puff). Fig. 5 shows comparison of j_s^{Xp} ratio for the cases of gas puff from the main plasma top (main-puff) and the divertor-puff at the same $\bar{n}_e$ of 2.75×10^{19} m^{-3}. Plasma detached near the separatrix (0–30 mm) during *x*-point MARFE, where $j_{s,up}^{Xp}$ and T_e^{Xp} profiles are identical for the two cases. Values of $j_{s,down}^{Xp}$ in the private flux and separatrix for the divertor-puff are by a factor of two larger than that for the main-puff case, and the flow reversal extended to the *x*-point. The plasma pressure at the down-stream increases due to the divertor-puff. This is consistent with the neutral pressures measured with fast ion gauges at the private flux region [8]. Neutral pressures at inner-side dome, outer-side dome and dome top are 1.7, 2.5 and 0.32 Pa for the divertor-puff, respectively, which are larger than those for the main-puff (i.e., 1.2, 1.6 and 0.18 Pa, respectively). Since plasma detachment extends to the *x*-point and to the outer radius, neutral density at the dome top is increased proportional to those at the dome sides.

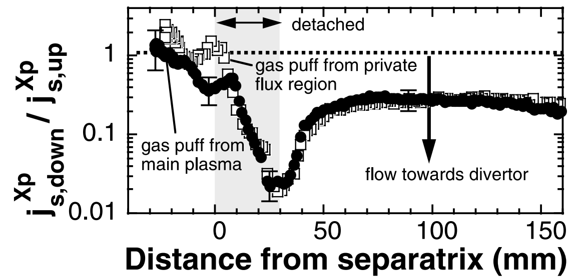

Fig. 5. Comparisons of j_s^{Xp} ratio for gas puff from main plasma (circles) and private flux region (squares). The measurements are taken during the *x*-point MARFE, and $\bar{n}_e = 2.75 \times 10^{19}$ m^{-3} during both-sides pumping.

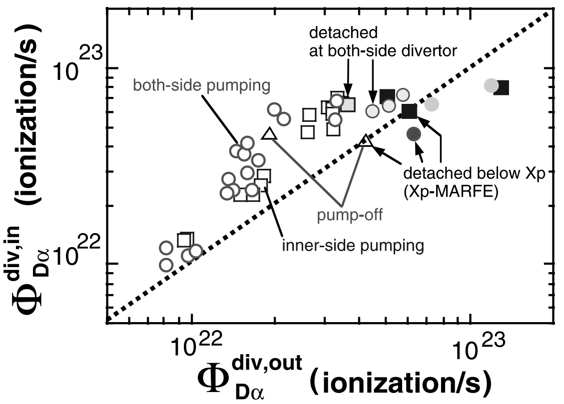

Fig. 6. Recycling fluxes in the inner and outer divertor, $\Phi_{D_\alpha}^{div,in}$ and $\Phi_{D_\alpha}^{div,out}$ for both-sides pumping (circles), inner-side pumping (squares), and pump-off cases (triangles). Attached divertor (including inner divertor detached), both-sides detached divertor and during x-point MARFE are shown by open, gray and black symbols, respectively.

4. In–out asymmetry in divertor recycling

In–out asymmetry in the particle recycling is compared in order to investigate effect of bypath between the inner and outer divertors. Recycling fluxes in the inner and outer divertors, $\Phi_{D_\alpha}^{div,in}$ and $\Phi_{D_\alpha}^{div,out}$, evaluated from (proportional to) the neutral deuterium line (D_α) brightness measurement using the photon emission rate coefficient by neutral ionization [9], are shown in Fig. 6. The evaluation of the recycling fluxes is only valid for the attached divertor. Recycling flux is increased with increasing $\bar{n}_e$, provided for attached divertor condition. Due to a larger ion flux to the inner divertor, $\Phi_{D_\alpha}^{div,in}$ is enhanced 2–3 larger than $\Phi_{D_\alpha}^{div,out}$. Recycling fluxes in the divertor and the in–out asymmetry are similar for the inner-side and both-sides pumping cases. Neutrals from the inner divertor to outer divertor through the bypath is small so that the in–out asymmetry does not change.

When plasma detachment occurs at the inner divertor separatrix, $\Phi_{D_\alpha}^{div,out}$ increases with $\bar{n}_e$, and then outer divertor plasma is detached. For the detached divertor without causing x-point MARFE, in–out symmetries in the D_α brightness profile, neutral pressure and ion flux are observed. Here, the radiation fractions in the divertor at the onset of the x-point MARFE are similar ($\sim$70% of P_{SOL}, where $P_{SOL} = P_{abs} - P_{rad}^{main}$) for the three cases. The both-sides pumping is favorable to increase the pumping rate and to improve impurity retention in the divertor.

5. Summary

With application of inner- and outer-divertor pumping, neutral flux from the inner divertor to outer divertor through under-dome is so small that the in–out asymmetry of the neutral recycling did not change. The plasma flow pattern did not change: flow reversal at outer midplane and flow towards the divertor at x-point with the ion ∇B drift towards the divertor. However, in the partially detached divertor, an increase in the plasma flow at the x-point was amplified by a reduction in the down-stream plasma pressure using pumping from the private flux region. Pumping at both-sides of the divertor was favorable for the partially detached plasma, which can be maintained without appearance of x-point MARFE and with in–out symmetrical profiles of particle recycling.

Acknowledgements

Authors thank Dr M. Shimada for very useful comments.

References

[1] K. Shimizu et al., J. Nucl. Mater. 241–243 (1997) 167.
[2] R. Monk et al., I-1.3 in PSI14.
[3] S.L. Allen et al., J. Nucl. Mater. 266–269 (1999) 168.
[4] R. Schneider et al., J. Nucl. Mater. 266–269 (1999) 175.
[5] N. Hosogane et al., J. Nucl. Mater. 266–269 (1999) 296.
[6] N. Asakura et al., Nucl. Fusion 39 (1999) 1983.
[7] N. Asakura et al., Phys. Rev. Lett. 84 (2000) 3093.
[8] H. Tamai et al., J. Plasma Fusion Res. 74 (1998) 1336.
[9] L.C. Johnson, E. Hinnov, J. Quant. Spectros. Radiat. Transfer 13 (1973) 311.